Intrinsic correlations among characteristics of neutron-rich matter imposed by the unbound nature of pure neutron matter

Bao-Jun Cai[1,*] and Bao-An Li[2,†]
[1]*Quantum Machine Learning Laboratory, Shadow Creator Inc., Shanghai 201208, China*
[2]*Department of Physics and Astronomy, Texas A&M University-Commerce, Commerce, Texas 75429-3011, USA*

(Received 2 December 2020; accepted 1 March 2021; published 11 March 2021)

Background: The equation of state (EOS) $E(\rho,\delta)$ of neutron-rich nucleonic matter at density ρ and isospin asymmetry δ can be approximated as the sum of the symmetric nuclear matter (SNM) EOS $E_0(\rho)$ and a power series in δ^2 with the coefficient $E_{\rm sym}(\rho)$ of its first term the so-called nuclear symmetry energy. Great effort has been devoted to studying the characteristics of both the SNM EOS $E_0(\rho)$ and the symmetry energy $E_{\rm sym}(\rho)$ using various experiments and theories over the last few decades. While much progress has been made in constraining parameters characterizing $E_0(\rho)$ and $E_{\rm sym}(\rho)$ around the saturation density ρ_0 of the SNM, such as the incompressibility K_0 of the SNM EOS as well as the magnitude S and the slope L of the nuclear symmetry, the parameters characterizing the high-density behaviors of both $E_0(\rho)$ and $E_{\rm sym}(\rho)$, such as the skewness J_0 and the kurtosis I_0 of the SNM EOS as well as the curvature $K_{\rm sym}$ and the skewness $J_{\rm sym}$ of the symmetry energy are still poorly known. Moreover, most attention has been put on constraining the characteristics of the SNM EOS and the symmetry energy separately as if $E_0(\rho)$ and $E_{\rm sym}(\rho)$ are completely independent.
Purpose: Because the EOS of pure neutron matter (PNM) is the sum of the SNM EOS and all the symmetry energy coefficients in expanding the $E(\rho,\delta)$ as a power series in δ^2, the unbound nature of PNM requires intrinsic correlations between the SNM EOS parameters and those characterizing the symmetry energy independent of any nuclear many-body theory. We investigate these intrinsic correlations and their applications in better constraining the poorly known high-density behavior of nuclear symmetry energy.
Method: We first derive an expression for the saturation density $\rho_{\rm sat}(\delta)$ of neutron-rich matter up to order δ^6 in terms of the EOS parameters. Setting $\rho_{\rm sat}(\delta)=0$ for PNM as required by its unbound nature leads to a sum rule for the EOS parameters. We then analyze this sum rule at different orders in δ^2 to find approximate expressions of the high-density symmetry energy parameters in terms of the relatively better determined SNM EOS parameters and the symmetry energy around ρ_0.
Results: Several novel correlations connecting the characteristics of the SNM EOS with those of nuclear symmetry energy are found. In particular, at the lowest-order of approximations, the bulk parts of the slope L, the curvature $K_{\rm sym}$, and the skewness $J_{\rm sym}$ of the symmetry energy are found to be $L\approx K_0/3$, $K_{\rm sym}\approx LJ_0/2K_0$, and $J_{\rm sym}\approx I_0L/3K_0$, respectively. High-order corrections to these simple relations can be written in terms of the small ratios of high-order EOS parameters. The resulting intrinsic correlations among some of the EOS parameters reproduce very nicely their relations predicted by various microscopic nuclear many-body theories and phenomenological models constrained by available data of terrestrial experiments and astrophysical observations in the literature.
Conclusion: The unbound nature of PNM is fundamental and the required intrinsic correlations among the EOS parameters characterizing both the SNM EOS and the symmetry energy are universal. These intrinsic correlations provide a novel and model-independent tool not only for consistency checks but also for investigating the poorly known high-density properties of neutron-rich matter by using those with smaller uncertainties.

DOI: 10.1103/PhysRevC.103.034607

I. INTRODUCTION

The equation of state (EOS) of cold asymmetric nucleonic matter (ANM) given in terms of the energy per nucleon $E(\rho,\delta)$ at density ρ and isospin asymmetry $\delta\equiv(\rho_n-\rho_p)/\rho$ between neutron and proton densities ρ_n and ρ_p is a fundamental quantity in nuclear physics and a basic input for various applications especially in astrophysics [1]. $E(\rho,\delta)$ is often expanded around $\delta=0$ to further define the EOS $E_0(\rho)$ of symmetric nucleonic matter (SNM) and various orders of the so-called nuclear symmetry energy according to

$$E(\rho,\delta)=E_0(\rho)+\sum_{i=1}^{\infty}E_{{\rm sym},2i}(\rho)\delta^{2i}. \quad (1)$$

Setting $\delta=1$, the above equation reduces to an approximate relation among the EOS $E_{\rm PNM}(\rho)\equiv E(\rho,1)$ of pure neutron matter (PNM), the SNM EOS $E_0(\rho)$, and all of the symmetry

*bjcai87@gmail.com
†Bao-An.Li@tamuc.edu

energy terms, i.e., $E_{\rm PNM}(\rho)=E_0(\rho)+\sum_{i=1}^{\infty}E_{{\rm sym},2i}(\rho)$. Normally the expansion in δ ends at the quadratic term with $i=1$ in the so-called parabolic approximation, and one generally refers the $E_{{\rm sym},2}(\rho)\equiv E_{\rm sym}(\rho)$ as the symmetry energy by neglecting all higher-order terms. One then expands the SNM EOS $E_0(\rho)$ and the symmetry energy $E_{\rm sym}(\rho)$ around the saturation density ρ_0 of the SNM with their characteristic coefficients, e.g., the incompressibility K_0, the skewness J_0, and the kurtosis I_0 of SNM as well as the magnitude S, the slope L, the curvature $K_{\rm sym}$, and the skewness $J_{\rm sym}$ of the symmetry energy $E_{\rm sym}(\rho)$.

Much effort in both experiments and theories has been devoted to investigating the characteristics of SNM during the past four decades and those of the symmetry energy over the past two decades, respectively. Indeed, much progress has been made in constraining both $E_0(\rho)$ and nuclear symmetry energy especially around and below ρ_0 (see, e.g., Refs. [2–9] for reviews). On the other hand, much progress has also been made in recent years in understanding properties of low-density PNM using state-of-the-art microscopic nuclear many-body theories and advanced computational techniques, e.g., chiral effective field theories [10] and quantum Monte Carlo techniques [11]. All calculations indicate that both the energy and the pressure in PNM approach zero smoothly and monotonically as the density vanishes, reflecting the unbound nature of PNM [12–16]. Moreover, it has been shown that the unitary Fermi gas EOS $E_{\rm UG}(\rho)=\xi E_{\rm FG}(\rho)$ in terms of the EOS of a free Fermi gas for neutrons, $E_{\rm FG}(\rho)$, and a Bertsch parameter of $\xi\approx 0.376$ [17] provides a lower bound to $E_{\rm PNM}(\rho)$ at low densities [18], demonstrating vividly the deep quantum nature of the system in the so-called contact region [19].

Imposing constraints on theories or fitting model predictions with experimental observables will naturally introduce correlations among the EOS parameters. Indeed, some interesting correlations have been found especially among the characteristics of either the SNM EOS $E_0(\rho)$ or the symmetry energy $E_{\rm sym}(\rho)$. It is also interesting to note that the low-density PNM EOS from the microscopic theories has been used as a boundary condition to calibrate some phenomenological models [20–22] and to explore some correlations among the EOS parameters [23,24]. In particular, the condition that the energy per neutron in PNM vanishes at zero density naturally leads to a linear correlation between $K_{\rm sym}$ and $3S$-L [25]. However, most of the correlations among the EOS parameters found so far are very model dependent, especially those involving the high-order coefficients (see, e.g., Refs. [6,18,25–32]). Because these correlations are known to have significant effects on properties of both nuclei and neutron stars (see, e.g., Refs. [23,26,33]), a better understanding of the correlations among the EOS parameters has significant ramifications in both nuclear physics and astrophysics.

In this work, we show that the unbound nature of PNM alone, especially its vanishing pressure P at zero density (i.e., the saturation density of ANM approaches zero as $\delta\to 1$), naturally leads to a sum rule linking intrinsically the EOS parameters independent of any theory. Analyses of this sum rule at different orders of the expansions in δ and ρ lead to novel correlations relating the characteristics of the SNM EOS with those of nuclear symmetry energy. In particular, at the lowest-order of approximations, we found that $L\approx K_0/3$, $K_{\rm sym}\approx LJ_0/2K_0$, and $J_{\rm sym}\approx I_0L/3K_0$, respectively. Corrections to these simple relations by considering high-order terms reproduce nicely the empirical correlations among some of the EOS parameters reported previously in the literature.

The rest of the paper is organized as follows. In Sec. II A, we recall the basic definitions of ANM EOS parameters. Intrinsic correlations among the EOS parameters and their general implications are given in Sec. II B. We then discuss potential applications of the intrinsic correlations. As the first example, we give in Sec. III A a scheme for estimating the slope L of the nuclear symmetry energy. Section III B is devoted to investigating the correlation between the curvature $K_{\rm sym}$ of the symmetry energy and L, K_0, and J_0. Relevant comparisons with the empirical $K_{\rm sym}$-L relations in the literature are also given in this section. In Secs. III D and III C, two direct implications of the $K_{\rm sym}$-L relation on the correlation between L and the symmetry energy magnitude S at ρ_0 as well as the isospin-dependent part of the incompressibility coefficient $K_{{\rm sat},2}$ are studied. Section III E gives a possible constraint on the skewness $J_{\rm sym}$ of the symmetry energy. A short summary is finally given in Sec. IV.

II. UNIVERSAL CONSTRAINTS ON THE EOS PARAMETERS OF NEUTRON-RICH MATTER BY THE UNBOUND NATURE OF PURE NEUTRON MATTER

A. Characteristics of isospin asymmetric nuclear matter

For ease of our discussions in the following, we summarize here the necessary notations and recall some terminologies we have adopted. Using δ and $\chi=(\rho-\rho_0)/3\rho_0$ as two perturbative variables, the EOS of ANM can be expanded around SNM at ρ_0 generally as $E(\rho,\delta)=w_{ij}\delta^{2i}\chi^j$, where the repeated indices are summed over, with each term characterized by $\delta^{2i}\chi^j$. In the following, we call "$2i+j$" the order of the quantity considered [34]. In this sense, $E_0(\rho_0)=w_{00}$ is the only zeroth-order term from $i=j=0$, and the first-order term is absent due to the vanishing pressure at ρ_0 in SNM by definition of its saturation point. At second order, we have $K_0=9\rho_0^2E_0''(\rho_0)=2w_{02}$ as well as $S\equiv E_{\rm sym}(\rho_0)=w_{10}$. Very similarly, we have at third order $L=3\rho_0E_{\rm sym}'(\rho_0)=w_{11}$ and $J_0=27\rho_0^3E_0'''(\rho_0)=6w_{03}$. While at fourth order, we have $I_0=81\rho_0^4E_0''''(\rho_0)=24w_{04}$, $K_{\rm sym}=9\rho_0^2E_{\rm sym}''(\rho_0)=2w_{12}$, and $S_4\equiv E_{{\rm sym},4}(\rho_0)=w_{20}$. Finally, the skewness $J_{\rm sym}=27\rho_0^3E_{\rm sym}'''(\rho_0)=6w_{13}$ of the symmetry energy $E_{\rm sym}(\rho)$ and the slope coefficient $L_{{\rm sym},4}=3\rho_0E_{{\rm sym},4}'(\rho_0)=w_{21}$ of the fourth-order symmetry energy $E_{{\rm sym},4}(\rho)$ are both at order 5.

B. Intrinsic correlations of EOS parameters and their general implications

The saturation density $\rho_{\rm sat}(\delta)$ for ANM with isospin asymmetry δ is defined as the point where the pressure vanishes, namely, $P[\rho_{\rm sat}(\delta)]=0$, or equivalently $\partial E(\rho,\delta)/\partial\rho|_{\rho=\rho_{\rm sat}(\delta)}=0$. After a long but straightforward calculation by expanding all the terms in Eq. (1) as functions of χ and the saturation density $\rho_{\rm sat}$ as a function of δ (see the

Appendix in Ref. [35]), one can obtain

$$\rho_{\rm sat}(\delta)/\rho_0 \approx 1+\Psi_2\delta^2+\Psi_4\delta^4+\Psi_6\delta^6+O(\delta^8), \quad (2)$$

with

$$\Psi_2 = -\frac{3L}{K_0}, \quad (3)$$

$$\Psi_4 = \frac{3K_{\rm sym}L}{K_0^2}-\frac{3L_{\rm sym,4}}{K_0}-\frac{3J_0L^2}{2K_0^3}, \quad (4)$$

$$\Psi_6 = \left(\frac{3K_{\rm sym}L}{K_0^2}-\frac{3J_0L^2}{2K_0^3}-\frac{3L_{\rm sym,4}}{K_0}\right)\left(\frac{J_0L}{K_0^2}-\frac{K_{\rm sym}}{K_0}\right) + \frac{I_0L^3}{2K_0^4}-\frac{3J_{\rm sym}L^2}{2K_0^3}+\frac{3K_{\rm sym,4}L}{K_0^2}-\frac{3L_{\rm sym,6}}{K_0}, \quad (5)$$

where $K_{\rm sym,4}$ is the curvature of the fourth-order symmetry energy and $L_{\rm sym,6}$ is the slope of the sixth-order symmetry energy. The expressions for Ψ_2 and Ψ_4 were first given in Ref. [35].

Required by the unbound nature of PNM as shown by all existing nuclear many-body theories, the saturation density of ANM eventually decreases from ρ_0 to zero as δ goes from 0 (SNM) to 1 (PNM). Quantitatively, to the order δ^6 this boundary condition requires $1+\Psi_2+\Psi_4+\Psi_6=0$. It can be rewritten using the characteristic EOS coefficients as an approximate sum rule:

$$1 = \frac{3L}{K_0}-\left(\frac{3K_{\rm sym}L}{K_0^2}-\frac{3J_0L^2}{2K_0^3}+\frac{3L_{\rm sym,4}}{K_0}\right)\left(1+\frac{J_0L}{K_0^2}+\frac{K_{\rm sym}}{K_0}\right) - \frac{I_0L^3}{2K_0^4}+\frac{3J_{\rm sym}L^2}{2K_0^3}-\frac{3K_{\rm sym,4}L}{K_0^2}+\frac{3L_{\rm sym,6}}{K_0}. \quad (6)$$

Clearly, it establishes an intrinsic correlation among the EOS parameters. Compared to the equation one would obtain from setting the energy per neutron $E_{\rm PNM}(0)=0$ at zero density, through couplings between isospin-independent and isospin-dependent coefficients the above relation provides a more stringent constraint for the high-order EOS parameters without involving the binding energy $E_0(\rho_0)$ of the SNM and the magnitude S of the symmetry energy at ρ_0. In fact, the latter has been well determined to be around $S=E_{\rm sym}(\rho_0)=31.7\pm3.2$ MeV by extensive analyses of terrestrial experiments and astrophysical observations [8,36] as well as *ab initio* nuclear-many theory predictions [37].

The analytic expressions for the saturation density at different orders of δ^2 characterized by Ψ_2, Ψ_4, and Ψ_6, etc., are very useful because they fundamentally encapsulate the intrinsic correlations among the characteristic EOS parameters. In this sense, intrinsic equations at different orders of δ^2 could be obtained. Specifically, if one truncates the saturation density $\rho_{\rm sat}^{\rm PNM}/\rho_0$ in PNM to order δ^2, an intrinsic equation of $1+\Psi_2=0$ is obtained. More accurately this should be an intrinsic inequality of $0\lesssim 1+\Psi_2\lesssim 1$. However, it is known that at the lowest orders of δ^2 in the so-called parabolic approximation, $\rho_{\rm sat}^{\rm PNM}$ is not necessarily zero in some of the many-body calculations (see examples given in Ref. [38]). Nevertheless, Eq. (2) provides a scheme to improve gradually the accuracy of calculating the saturation density of ANM. For example, the intrinsic equation $1+\Psi_2+\Psi_4=0$ or $1+\Psi_2+\Psi_4+\Psi_6=0$ could be obtained if $\rho_{\rm sat}^{\rm PNM}/\rho_0$ is truncated at order δ^4 or δ^6, respectively. As the order of truncation increases, the quantity $1+\sum_{j=1}\Psi_{2j}=1+\Psi_2+\Psi_4+\cdots$ becomes more and more close to 0, and the intrinsic correlations or the sum rule $1+\sum_{j=1}\Psi_{2j}=0$ obtained becomes more and more accurate. Moreover, as the accuracy in estimating $\rho_{\rm sat}(\delta)$ increases, more high-order EOS parameters get involved, as one would expect.

We point out the following two basic usages of the intrinsic equations (at different orders of δ^2).

(i) The intrinsic equations can be effectively used to establish useful connections between parameters characterizing the SNM EOS and those describing the symmetry energy. For example, one can immediately obtain from the intrinsic equation $1+\Psi_2=0$ at order δ^2 the relation $L\approx K_0/3$, and if the coefficient K_0 is better constrained, then the L coefficient can be subsequently inferred. Moreover, if both of them are independently determined, this simple relation allows for a consistency check. Naturally, if higher-order contributions are included, this simple relation is expected to be modified. In Sec. III A, we investigate this issue in more detail. The most important physics outcome is that the approximate relations, e.g., $L\approx K_0/3$, provide a useful guide for developing phenomenological models and microscopic theories.

(ii) As mentioned above, as the truncation order of the expansion (2) increases, more and more characteristic coefficients will be included; i.e., they will emerge in the intrinsic equations as the order increases. Then, the correlations can potentially allow one to extract high-order (poorly known) coefficients from the lower-order (better known) ones. An example given in Sec. III B on extracting $K_{\rm sym}$ from its correlation with L demonstrates this point in detail.

Moreover, a few interesting points related to Eqs. (2) and (6) are worth emphasizing.

(i) Because the saturation density $\rho_{\rm sat}(\delta)/\rho_0$ is obtained order by order, one naturally expects that the higher-order term contributes less. If $\rho_{\rm sat}(\delta)/\rho_0$ is truncated at order δ^2, then one has $\Psi_2=-1$. Actually what we have obtained is $0\gtrsim\Psi_2\gtrsim-1$. Next if the Ψ_4 contribution is taken into consideration, we have $\rho_{\rm sat}^{\rm PNM}/\rho_0=1+\Psi_2+\Psi_4=0$, i.e., $\Psi_2=-1-\Psi_4$. Simultaneously setting $|\Psi_2|\lesssim 1$ and $|\Psi_4|\lesssim|\Psi_2|$ gives the constraint on Ψ_4 as $-1/2\lesssim\Psi_4\lesssim 0$. When the Ψ_6 term is included, a similar analysis on the value of Ψ_6 can be made.

(ii) Although Eq. (6) implies a complicated intrinsic correlation among all the parameters involved, certain terms could directly be found to be less important. For example, the characteristic coefficients related to the fourth-order symmetry energy $E_{\rm sym,4}(\rho)$, namely, $L_{\rm sym,4}$ and $K_{\rm sym,4}$, are expected to be small, because the value of $S_4\equiv E_{\rm sym,4}(\rho_0)$ is known to be smaller than about 2 MeV [39–42]. Particularly, by adopting a density dependence similar to the symmetry energy

$E_{\rm sym}(\rho)$ [43] as $E_{\rm sym,4}(\rho) = S_4(\rho/\rho_0)^\gamma$, with γ being an effective density-dependence parameter, one obtains $L_{\rm sym,4} = 3\gamma S_4$ and $K_{\rm sym,4} \approx 9\gamma(\gamma-1)S_4$. A conservative estimate with $0 \lesssim \gamma \lesssim 2$ indicates that $0\ {\rm MeV} \lesssim L_{\rm sym,4} \lesssim 12$ MeV and $-4.5\ {\rm MeV} \lesssim K_{\rm sym,4} \lesssim 36$ MeV. Consequently, one can safely neglect the term "$-3K_{\rm sym,4}L/2K_0^3$" in Eq. (6) because its magnitude is smaller than 1.5% with the currently known most probable values of L [8,36] and K_0 [9]. For similar reasons, the last term in Eq. (6) involving the slope $L_{\rm sym,6}$ of the six-order symmetry energy $E_{\rm sym,6}(\rho)$ can also be neglected. However, the term involving $L_{\rm sym,4}$ might be important and it is kept in the following discussions.

(iii) By truncating Eq. (2) at different orders of δ^2, different intrinsic correlation equations are obtained, but they are not all independent. As the truncation order increases, the intrinsic correlation becomes more general because more and more characteristic coefficients are taken into consideration. Of course, the resulting dependencies and correlations among the EOS parameters look gradually more complicated.

III. APPLICATIONS OF THE INTRINSIC CORRELATIONS AMONG EOS PARAMETERS

In this section, we present a few applications of the sum rule in Eq. (6) at different orders of δ^2. To justify some of our numerical approximations and for ease of our discussions, it is useful to note here the currently known ranges of the lower-order parameters and the rough magnitudes of the high-order parameters. In particular, we use the empirical values of $K_0 \approx 240 \pm 20$ MeV [6,9,44–46], $J_0 \approx -300$ MeV [34], and $I_0 \approx -146 \pm 1728$ MeV [47] for the SNM EOS. For the symmetry energy, it is known that $L \approx 60 \pm 30$ MeV [36], $K_{\rm sym} \approx -80$ MeV [48], and $J_{\rm sym} \approx 300$ MeV [29]. While the community has not reached a consensus on the exact ranges of some of the high-order parameters, the reference values enable us to make rough estimates and judge if some of the ratios and terms in our analyses can be neglected.

A. Estimating the slope L of nuclear symmetry energy

As the first application of the intrinsic equations, we derive an expression for the slope L of the symmetry energy in terms of better known quantities corrected by some ratios of other parameters that are small. The main purpose of this analysis is to show how the unbound nature of PNM naturally gives a good estimate for L.

As discussed in Sec. II B, the intrinsic equation at order δ^2 gives the lowest-order approximation $L \approx K_0/3$. Thus, by introducing the dimensionless quantity $x = 3L/K_0$ (consequently $x^{(0)} \approx 1$ corresponding to $L \approx K_0/3$ could be found) and the following combinations,

$$\psi_0 = 1 - \frac{3L_{\rm sym,4}}{K_0} - \frac{3L_{\rm sym,6}}{K_0}, \tag{7}$$

$$\psi_1 = 1 - \frac{K_{\rm sym}}{K_0} + \frac{L_{\rm sym,4}J_0}{K_0^2} - \frac{K_{\rm sym,4}}{K_0} + \frac{K_{\rm sym}^2}{K_0^2}, \tag{8}$$

$$\psi_2 = 1 - \frac{3K_{\rm sym}}{K_0} + \frac{J_{\rm sym}}{J_0}, \tag{9}$$

$$\psi_3 = 1 - \frac{3J_0^2}{K_0 I_0}, \tag{10}$$

we obtain the equation for x by rewriting Eq. (6) as

$$\psi_0 - \psi_1 x - \frac{1}{6}\frac{J_0}{K_0}\psi_2 x^2 + \frac{1}{54}\frac{I_0}{K_0}\psi_3 x^3 = 0. \tag{11}$$

Rewriting Eq. (6) in the form (11) is mainly for the convenience of discussing its relevance for estimating L. If on the other hand the interested quantity is $K_{\rm sym}$, then Eq. (6) can be cast into the form $AK_{\rm sym}^2 + BK_{\rm sym} + C = 0$ with A, B, and C being some relevant coefficients independent of $K_{\rm sym}$. We note that J_0 appearing in ψ_1 comes from Ψ_4, while $J_{\rm sym}$ and I_0 appearing in ψ_2 and ψ_3 come from Ψ_6.

Different approximations of Eq. (11) and analysis can developed. In the following, we discuss approximate solutions of Eq. (11) at δ^2, δ^4, and δ^6 orders, separately. At the δ^2 order, besides the simplest estimation $L \approx K_0/3$ by taking $\psi_0 \approx \psi_1 \approx 1$ in Eq. (11) and simultaneously neglecting the x^2 and x^3 terms, one can also find that $L/K_0 > 0$, i.e., the sign of the incompressibility K_0 is the same as that of the slope L. The latter can be seen from the relation $\rho_{\rm sat}(\delta)/\rho_0 \approx 1 + \Psi_2\delta^2 + O(\delta^4)$ and $\Psi_2 = -3L/K_0$. As the isospin asymmetry δ increases from 0 to a small finite value, the saturation density has to be reduced. Thus, Ψ_2 has to be negative, requiring $L/K_0 > 0$.

Systematically, we can generalize the relation $L \approx K_0/3$ as

$$L \approx \frac{K_0}{3}(1 + \text{"higher-order corrections"}), \tag{12}$$

when the higher-order terms $\Psi_4\delta^4$, $\Psi_6\delta^6$, etc., are taken into account in the saturation density $\rho_{\rm sat}/\rho_0$. For example, at the δ^4 order, by considering the Ψ_4 term, but simultaneously neglecting the Ψ_6 term, the coefficients related to the fourth-order symmetry energy, and the small terms $(K_{\rm sym}/K_0)^2$ and $J_0K_{\rm sym}/2K_0^2$, one can obtain

$$\frac{1}{6}\frac{J_0}{K_0}x^2 + \left(1 - \frac{K_{\rm sym}}{K_0}\right)x - 1 = 0. \tag{13}$$

Its solution leads to

$$L = \left(1 - \frac{K_{\rm sym}}{K_0}\right)\frac{K_0^2}{J_0}\left[\sqrt{1 + \frac{2}{3}\frac{J_0}{K_0}\left(1 - \frac{K_{\rm sym}}{K_0}\right)^{-2}} - 1\right] \tag{14}$$

$$\approx \frac{K_0}{3}\left(1 - \frac{K_{\rm sym}}{K_0}\right)^{-1}\left[1 - \frac{1}{6}\frac{J_0}{K_0}\left(1 - \frac{K_{\rm sym}}{K_0}\right)^{-2}\right], \tag{15}$$

where the second approximation is obtained by noticing that $|1 + (2J_0/3K_0)(1 - K_{\rm sym}/K_0)^{-2}| \ll 1$ using the empirical values of the involved parameters given earlier. In addition, the positiveness of the discriminant of Eq. (13) limits the skewness J_0 to $J_0 \gtrsim -3K_0(1 - K_{\rm sym}/K_0)^2/2$. Because $K_{\rm sym}/K_0 \approx -1/3$ and $J_0/6K_0 \approx -5/24$ are both small and at the same level, the above expression for L can be further approximated as

$$L \approx \frac{K_0}{3}\left(1+\frac{K_{\rm sym}}{K_0}-\frac{1}{6}\frac{J_0}{K_0}\right). \tag{16}$$

Similarly, at the δ^6 order, again by neglecting the coefficients related to the fourth-order and the sixth-order symmetry energies as well as the other small terms, the solution of Eq. (11) leads to

$$L \approx \frac{K_0}{3}\left[1+\frac{K_{\rm sym}}{K_0}-\frac{J_0+J_{\rm sym}}{6K_0} + \frac{I_0}{54K_0}\left(1+\frac{4K_{\rm sym}}{K_0}-\frac{5J_0}{6K_0}+\frac{I_0}{18K_0}\right)\right]. \tag{17}$$

While the kurtosis I_0 and the incompressibility K_0 have similar orders of magnitude, the second line of Eq. (17) contributes only about 2% compared to the leading contribution "1." Using the empirical values of the EOS parameters given earlier, the "high-order contribution" in Eq. (17) is estimated to be about -33%. Consequently, L is about 53.3 MeV, compared to the simplest estimation of about 80 MeV from $L \approx K_0/3$. Moreover, the coefficient $1/54$ together with the small ratios enable us to further approximate the expression (17) as

$$L \approx \frac{K_0}{3}\left(1+\frac{K_{\rm sym}}{K_0}-\frac{1}{6}\frac{J_0}{K_0}-\frac{1}{6}\frac{J_{\rm sym}}{K_0}+\frac{1}{54}\frac{I_0}{K_0}\right). \tag{18}$$

As noticed before, $J_{\rm sym}$ and I_0 appear only in Ψ_6. Neglecting them, the above expression naturally reduces to Eq. (16) valid at the δ^4 order as one expects.

Our analyses above indicate clearly that as the truncation order of $\rho_{\rm sat}^{\rm PNM}$ increases, the higher-order terms become eventually irrelevant although they appear in a complicated manner. To understand the results intuitively, it is useful to look at the analogy with the period T of small-angle oscillations of a simple pendulum:

$$T(\theta) \approx 2\pi\sqrt{\frac{l}{g}}\left(1+\frac{1}{16}\theta^2+\frac{11}{3072}\theta^4\right), \tag{19}$$

where θ is the maximum angle and l is the length of the pendulum. For $\theta = 1$, we obtain from the above expression the period $T(1) \approx 1.066T(0)$. While the exact result is $T(1) \approx 1.085T(0)$, indicating that although the apparent perturbation element θ is not much smaller than 1, the perturbative expansion is still very effective (useful) near $\theta \approx 1$ due to the small in-front coefficients $1/16$ and $11/3072$ in the expansion of $T(\theta)$.

B. Intrinsic correlation between $K_{\rm sym}$ and L

Besides estimating the slope L, the intrinsic equations could also be used to investigate the correlations among certain EOS parameters. Because $K_{\rm sym}$ first appears at the δ^4 order in the Ψ_4 term, through the intrinsic equation $1+\Psi_2+\Psi_4 = 0$, we obtain the following relation for $K_{\rm sym}$,

$$K_{\rm sym} \approx K_0\left(1-\frac{1}{3}\frac{K_0}{L}+\frac{1}{2}\frac{J_0}{K_0}\frac{L}{K_0}+\frac{L_{\rm sym,4}}{L}\right). \tag{20}$$

One can first check the magnitude of $K_{\rm sym}$ using this equation. By taking $K_0 \approx 240$ MeV, $J_0 \approx -300$ MeV, $L \approx 60$ MeV, and $L_{\rm sym,4} \approx 6$ MeV, one obtains $K_{\rm sym} \approx -93$ MeV. In addition, if one assumes $|\Psi_4/\Psi_2| \lesssim 1$, then one finds -253 MeV $\lesssim K_{\rm sym} \lesssim 227$ MeV. These results are consistent with the constraint on $K_{\rm sym}$ obtained recently from Bayesian analyses of neutron star observations [48,49].

It is necessary to point out that the relations (14) or (15) and (20) are not independent, and in fact they are effectively two different presentations of the same intrinsic equation. However, they are usefully different in the sense that they give separately the expressions for L and $K_{\rm sym}$ in terms of their main parts plus small corrections determined by the ratios of other EOS parameters. The analysis above indicates that $K_{\rm sym}$ is closely correlated with K_0, L, and J_0 while $L_{\rm sym,4}/L$ has negligible effects as we discussed earlier. Moreover, taking the lowest-order approximation for L, i.e., $L \approx K_0/3$, the expression (20) can be further reduced to

$$K_{\rm sym} \approx K_0\left(\frac{1}{2}\frac{J_0}{K_0}\frac{L}{K_0}+\frac{L_{\rm sym,4}}{L}\right) \approx LJ_0/2K_0. \tag{21}$$

One then immediately finds qualitatively that $K_{\rm sym}$ correlates positively with L and J_0 but negatively with K_0.

In the following, we investigate more quantitatively the correlations of $K_{\rm sym}$ with other EOS parameters using the more accurate relation (20). For this purpose, we perform a Monte Carlo sampling of the EOS parameters in their currently known ranges. Shown in Fig. 1 are the correlations between $K_{\rm sym}$ and $L_{\rm sym,4}$, $K_{\rm sym}$ and L, $K_{\rm sym}$ and K_0, and $K_{\rm sym}$ and J_0, respectively. In this study, the parameters are randomly sampled simultaneously and uniformly in the ranges of 0 MeV $\lesssim L_{\rm sym,4} \lesssim 12$ MeV, 30 MeV $\lesssim L \lesssim$ 90 MeV, 200 MeV $\lesssim K_0 \lesssim 280$ MeV, and -500 MeV $\lesssim J_0 \lesssim$ -100 MeV. From the results shown we clearly observe that $K_{\rm sym}$ has weak positive correlations with both $L_{\rm sym,4}$ and J_0 but a strong positive (negative) correlation with L (K_0). When more experimental constraints on the EOS parameters become available, the accuracy and robustness of the correlations are expected to be improved. However, the correlation patterns revealed here should stay the same.

The strengths of correlations between $K_{\rm sym}$ and the other EOS parameters can be quantified using the quantity $\Theta(\phi_i) = \delta\phi_i\partial K_{\rm sym}/\partial\phi_i$, where $\phi_i = L_{\rm sym,4}, L, K_0$, and J_0. More specifically, we find that $\Theta(L) \approx 258$ MeV, $\Theta(L_{\rm sym,4}) \approx 32$ MeV, $\Theta(K_0) \approx -120$ MeV, and $\Theta(J_0) \approx 50$ MeV, respectively. These numbers clearly quantify the strengths of the correlations shown in Fig. 1. It is interesting to note here that the results of our model-independent analyses are very consistent with the findings of Ref. [25] (see Fig. 7 therein). In the latter, the correlations were obtained from some basic physical constraints imposed on the Taylor's expansion of the binding energy in ANM around ρ_0 [25]. One of the constraints Ref. [25] uses is that the EOS of PNM at zero density is 0. The present analysis thus shares with Ref. [25] the requirement that the PNM is unbound. However, as we pointed out earlier, the vanishing pressure of PNM puts more stringent constraints on the high-order EOS parameters than its vanishing binding energy at zero density.

The near-linear correlations between $K_{\rm sym}$ and the other EOS parameters can also be described more quantitatively. For example, the correlation between $K_{\rm sym}$ and L can be

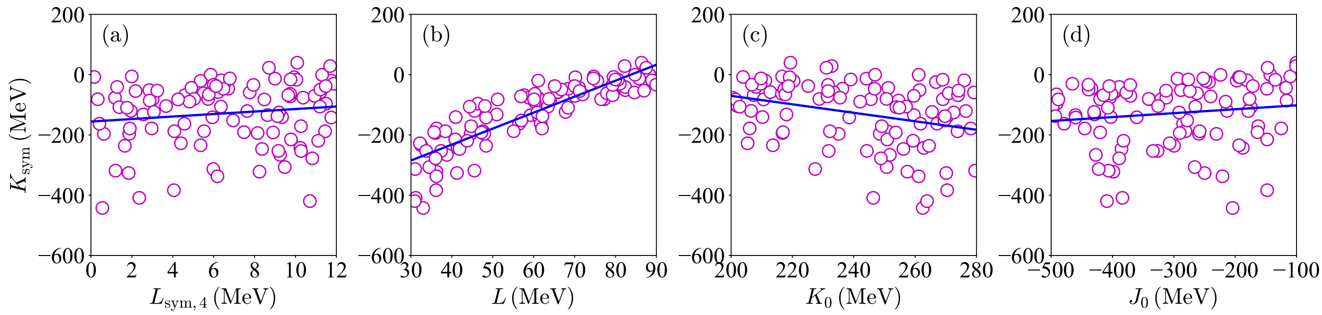

FIG. 1. Correlations between $K_{\rm sym}$ and $L_{\rm sym,4}$, L, K_0, and J_0 according to Eq. (20).

written as $K_{\rm sym} \approx a_1 L + b_1$. By minimizing the algebraic error, the coefficients a_1 and b_1 can be obtained as

$$a_1 \approx \frac{\langle K_{\rm sym} L\rangle - \langle K_{\rm sym}\rangle\langle L\rangle}{\langle L^2\rangle - \langle L\rangle^2} \tag{22}$$

and $b_1 = \langle K_{\rm sym}\rangle - a_1\langle L\rangle$, where the average $\langle\cdots\rangle$ for one independent simulation with total m points is defined simply as $\langle k\rangle = m^{-1}\sum_{i=1}^m k^{(i)}$. By independently sampling n times, one obtains the standard uncertainty of a_1 or b_1 as

$$\sigma_f = \sqrt{\frac{1}{n}\sum_{i=1}^n f^{(i),2} - \left(\frac{1}{n}\sum_{i=1}^n f^{(i)}\right)^2}, \tag{23}$$

where $f^{(i)} \leftrightarrow a_1^{(i)}, b_1^{(i)}$. Using $m = 10^2$ and $n = 10^4$ in our simulations, we find $\overline{a}_1 = n^{-1}\sum_{i=1}^n a_1^{(i)} \approx 5.25 \pm 0.40$ and similarly $\overline{b}_1 = n^{-1}\sum_{i=1}^n b_1^{(i)} \approx -441 \pm 28$ MeV. Taking $L \approx 60$ MeV in $K_{\rm sym} \approx \overline{a}_1 L + \overline{b}_1$ gives $K_{\rm sym} \approx -126$ MeV. For the correlation between $K_{\rm sym}$ and $L_{\rm sym,4}$, namely, $K_{\rm sym} \approx a_2 L_{\rm sym,4} + b_2$, one has $\overline{a}_2 \approx 4.42 \pm 3.11$ and $\overline{b}_2 \approx -152 \pm 22$ MeV, and similarly for $K_{\rm sym}$ and K_0, namely, $K_{\rm sym} \approx a_3 K_0 + b_3$, one has $\overline{a}_3 \approx -1.66 \pm 0.44$ and $\overline{b}_3 \approx 272 \pm 103$ MeV. Finally for the correlation between $K_{\rm sym}$ and J_0, i.e., $K_{\rm sym} \approx a_4 J_0 + b_4$, the results are found to be $\overline{a}_4 \approx 0.13 \pm 0.09$ and $\overline{b}_4 \approx -88 \pm 30$ MeV. It is necessary to point out that while the central values of $\overline{a}_i$ and $\overline{b}_i$ (with $i = 1$–4) will approach those determined by the central values of the characteristic coefficients, e.g., L and K_0, for the simulation as $n \to \infty$ according to the law of large numbers [50], the magnitude of the uncertainty is affected by the choice of m. A smaller m leads to a larger uncertainty as one would expect.

When high-order contributions are considered, we can similarly study the correlation between $K_{\rm sym}$ and the other EOS coefficients. For instance, at the δ^6 order, the relevant equation for calculations is obtained by neglecting the coefficients $L_{\rm sym,6}$ and $K_{\rm sym,4}$ in Eq. (6). Figure 2 shows results of a Monte Carlos sampling of the correlations at the δ^6 order using 0 MeV $\lesssim J_{\rm sym} \lesssim$ 2000 MeV and -2000 MeV $\lesssim I_0 \lesssim$ 2000 MeV as well as those ranges given earlier for the low-order EOS parameters. It is seen that the positive (negative) correlation between $K_{\rm sym}$ and L (K_0) is unchanged when the relevant higher-order contributions are included. This means that the qualitative features of the intrinsic correlations obtained earlier from Eq. (6) at the δ^4 order remain stable, while the fitting coefficients are affected quantitatively. More specifically, now for the correlation $K_{\rm sym} \approx a_1' L + b_1'$ the n averages of a_1' and b_1' are found to be $\overline{a}_1' \approx 3.61 \pm 0.43$ and $\overline{b}_1' \approx -268 \pm 21$ MeV, respectively. Similarly for the correlation $K_{\rm sym} \approx a_3' K_0 + b_3'$, we have $\overline{a}_3' \approx -0.75 \pm 0.30$ and $\overline{b}_3' \approx 90 \pm 71$ MeV, respectively.

It is also interesting to compare our $K_{\rm sym}$-L correlation with typical results obtained from other approaches in the literature [18,29,30]. More specifically, Ref. [29] gave a correlation of $K_{\rm sym} \approx (-4.97 \pm 0.07)(3S - L) + 67 \pm 2$ MeV at 68% confidence level from analyzing over 520 predictions of the Skyrme-Hartree-Fock energy density functionals and the relativistic mean-field theories. Their result using $S \approx 32 \pm 3$ MeV is shown with the black lines in Fig. 3. The authors of Ref. [18] did an analysis similar to that of Ref. [29] but applied additional constraints. Their result $K_{\rm sym} \approx 3.50L - 306 \pm 24$ MeV is shown as the sky blue band in Fig. 3. In Ref. [30], a $K_{\rm sym}$-L correlation was derived by using the Fermi liquid theory with its parameters calibrated by the chiral effective field theory at subsaturation densities. Their correlation $K_{\rm sym} \approx 2.76L - 203 \pm 22$ MeV is shown as the cyan band. While our result is shown with the purple band. It is seen that our correlation is highly consistent with the results from the three other studies. They all overlap largely around the upper boundary from the analysis of Ref. [29]. More quantitatively, taking $L \approx 60$ MeV in $K_{\rm sym} \approx \overline{a}_1' L + \overline{b}_1'$ gives $K_{\rm sym} \approx -52$ MeV, while the same value of L leads to a mean value of $K_{\rm sym} \approx -112$, -96, and -37 MeV using the constraints from Refs. [18,29,30], respectively. We also notice

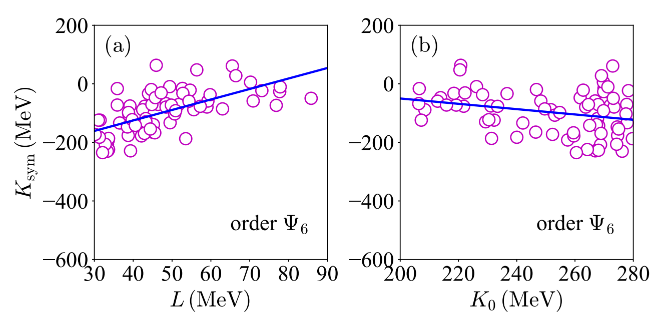

FIG. 2. Correlations between $K_{\rm sym}$ and L (left) and between $K_{\rm sym}$ and K_0 (right) to order Ψ_6.

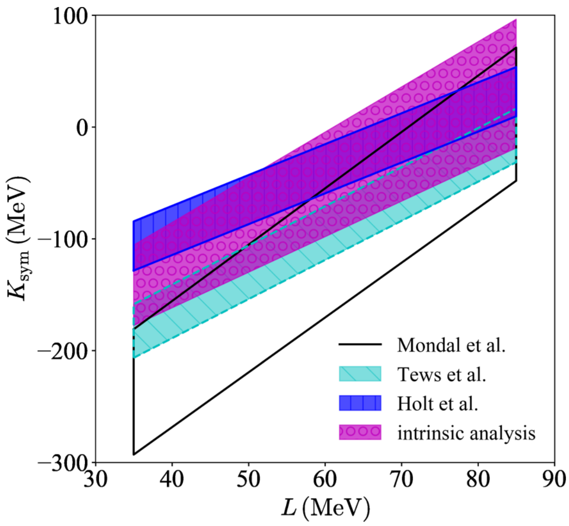

FIG. 3. Correlation between $K_{\rm sym}$ and L from intrinsic analysis as well as the prediction of it from Refs. [18,29,30].

that a very recent study based on the so-called KIDS energy functional [32] gave a $K_{\rm sym}$-L correlation consistent with the results discussed above. More quantitatively, they concluded that the curvature $K_{\rm sym}$ is probably negative and not lower than −200 MeV [32]. Finally, it is also interesting to note that the analysis combining the tidal deformability of neutron stars via a χ^2-based covariance approach also showed that the coefficients $K_{\rm sym}$ and L are strongly correlated [51,52].

C. Implications of the intrinsic $K_{\rm sym}$-L correlation on the incompressibility of neutron-rich matter along its saturation line

The incompressibility of neutron-rich matter

$$K_{\rm sat}(\delta) \equiv 9\rho_{\rm sat}^2 \frac{\partial^2 E(\rho,\delta)}{\partial\rho^2}\bigg|_{\rho=\rho_{\rm sat}} \approx K_0 + K_{\rm sat,2}\delta^2 + O(\delta^4) \tag{24}$$

is an important quantity directly related to the ongoing studies of various collective modes and the stability of neutron-rich nuclei [9]. The strength of its isospin-dependent part can be written as [35]

$$K_{\rm sat,2} = K_{\rm sym} - 6L - J_0L/K_0. \tag{25}$$

By using Eq. (20) for $K_{\rm sym}$, the latter can be rewritten as

$$K_{\rm sat,2} \approx \left(1 + \frac{L_{\rm sym,4}}{L} - \frac{K_0}{3L}\right)K_0 - \left(6 + \frac{J_0}{2K_0}\right)L. \tag{26}$$

Numerically, we find $K_{\rm sat,2} \approx -378$ MeV using the empirical values of the EOS parameters given earlier. This value is consistent with the latest study on $K_{\rm sat,2}$ within the KIDS framework where it was found that $K_{\rm sat,2}$ should roughly lie between −400 and −300 MeV [32]. Similar to what is shown in Fig. 1, using the above expression for $K_{\rm sat,2}$ one can also analyze its correlations with K_0, L, $L_{\rm sym,4}$, and J_0, separately. Moreover, noticing that $|L_{\rm sym,4}/L| \ll 1$ and $L \approx K_0/3$, $K_{\rm sat,2}$ can be further approximated as

$$K_{\rm sat,2} \approx -2K_0 - J_0/6. \tag{27}$$

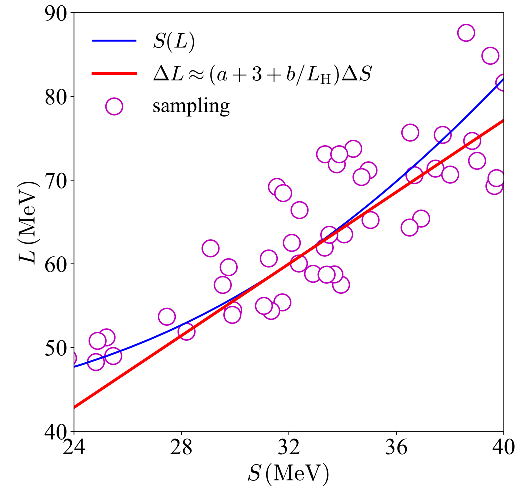

FIG. 4. Correlation between L and S.

This relation clearly demonstrates that the uncertainty of $K_{\rm sat,2}$ mainly comes from the poorly known J_0, although its contribution has a shrinking factor of −1/6.

D. Implications of the intrinsic $K_{\rm sym}$-L correlation on the L-S correlation of the symmetry energy

The near-linear correlation between $K_{\rm sym}$ and L also has an important implication for the correlation between L and S of the symmetry energy at ρ_0. Note that at an arbitrary density ρ

$$\frac{dL(\rho)}{dE_{\rm sym}(\rho)} = \frac{dL(\rho)}{d\rho}\bigg/\frac{dE_{\rm sym}(\rho)}{d\rho} = 3 + \frac{K_{\rm sym}(\rho)}{L(\rho)} \tag{28}$$

according to the basic definitions of the characteristic coefficients of the symmetry energy $E_{\rm sym}(\rho)$. By taking $\rho = \rho_0$, the relation (28) gives $dL/dS = 3 + K_{\rm sym}/L$. For instance, L and $K_{\rm sym}$ in the free Fermi gas model are $L = 2S$ and $K_{\rm sym} = -2S = -L$, respectively, automatically fulfilling the relation (28). Using the intrinsic correlation $K_{\rm sym} \approx aL + b$ found earlier and by integrating $\int dS = \int dL(3 + K_{\rm sym}/L)^{-1} = \int dL(a + 3 + b/L)^{-1}$, we obtain the following relation between S and L:

$$S(L) = \frac{1}{a+3}\left(L - \frac{b}{a+3}\ln\left[(a+3)L + b\right]\right) + \text{const.}, \tag{29}$$

where the constant is determined via some reference point $(S_{\rm H}, L_{\rm H})$, e.g., $S_{\rm H} \approx 32$ MeV and $L_{\rm H} \approx 60$ MeV at ρ_0 according to the surveys of available data [8,36].

Shown in Fig. 4 with the pink circles are the Monte Carlo samplings of the L-S correlation within the empirical EOS parameter ranges and adopting $\overline{a}_1' \approx 3.61$ and $\overline{b}_1' \approx -268$ MeV from the δ^6 order analysis discussed earlier. Due to the near-linear correlation between $K_{\rm sym}$ and L, the correlation between L and S is also found to be near linear, although it is not so obvious that the relation (29) is linear. Because the near linearity between $K_{\rm sym}$ and L is intrinsic (only the fitting coefficients vary if the intrinsic equation is truncated at different orders), the near linearity between L and S is also expected to be intrinsic. Specifically, one can easily show that

$$\Delta L \approx \Phi\Delta S\left[1-\left(b/2L_{\rm H}^2\right)\Delta S\right], \quad \Phi = a+3+b/L_{\rm H}, \quad (30)$$

where $\Delta L = L - L_{\rm H}$, $\Delta S = S - S_{\rm H}$, and Φ is simply the value of $3 + K_{\rm sym}/L$ taken at $L_{\rm H}$. Numerically, we obtain the relation $L \approx 2.14\Delta S + 0.08\Delta S^2 + L_{\rm H}$ by using $a = \overline{a}_1' \approx 3.61$ and $b = \overline{b}_1' \approx -268$ MeV. The quadratic correction $0.08\Delta S^2$ is small; thus $\Delta L \approx 2.14\Delta S$ and consequently $L \approx 2.14S - 8.6$ MeV, which is very close to the free Fermi gas model prediction of the L-S relation $L = 2S$. The resulting linearized ΔL-ΔS correlation (30) (by neglecting the ΔS^2 correction) and the full L-S correlation (29) are shown with the red and blue lines, respectively, in Fig. 4. Around the currently known most probable value of $S = E_{\rm sym}(\rho_0) = 31.7 \pm 3.2$ MeV [8,36], both the L-S and the Monte Carlo samplings are approximately linear consistently. Moreover, by putting L in terms of S back into the relation $K_{\rm sym} \approx aL + b$, we obtain $K_{\rm sym} \approx 7.74S - 299$ MeV, which has a large deviation from its free Fermi gas model counterpart (see also Ref. [30]).

E. Estimating the $K_{\rm sym}$-$J_{\rm sym}$ correlation

$J_{\rm sym}$ first emerges in Ψ_6; one can thus investigate its intrinsic correlations with the other EOS parameters starting from the order δ^6. Because it is a high-order parameter, its value is poorly known and some of its correlations especially with the low-order parameters are expected to be weak. Solving the intrinsic equation (6) by neglecting $L_{\rm sym,4}$, $K_{\rm sym,4}$, and $L_{\rm sym,6}$ leads to the following estimation for $J_{\rm sym}$:

$$J_{\rm sym} \approx \frac{2K_0^3}{3L^2}\left(1-\frac{3L}{K_0}\right) + \left(\frac{2K_0K_{\rm sym}}{L} - J_0\right)\left(1+\frac{J_0L}{K_0^2}-\frac{K_{\rm sym}}{K_0}\right) + \frac{I_0L}{3K_0}. \quad (31)$$

Taking the lowest-order approximations for $L \approx K_0/3$ and $K_{\rm sym} \approx LJ_0/2K_0$ obtained earlier, the above equation can be further reduced to $J_{\rm sym} \approx I_0L/3K_0$. Numerically, we have $J_{\rm sym} \approx 281$ MeV by putting the empirical values of K_0, J_0, I_0, L, and $K_{\rm sym}$ given earlier into Eq. (31). This value is consistent with the constraint $J_{\rm sym} \approx 296.8 \pm 73.6$ MeV from analyzing the systematics of over 520 energy density functionals in Ref. [29]. It is also consistent with $J_{\rm sym} = 90 \pm 334$ MeV at 68% confidence level from a recent Bayesian analysis in Ref. [53] (see Table 4 therein).

Figure 5 shows the $J_{\rm sym}$-$K_{\rm sym}$ correlation from our Monte Carlo samplings in the range of -400 MeV $\lesssim K_{\rm sym} \lesssim 0$ MeV while the other EOS parameters are taken randomly in their empirical ranges given earlier. It is seen that there is a strong correlation between $J_{\rm sym}$ and $K_{\rm sym}$. In fact, $J_{\rm sym}$ depends on $K_{\rm sym}$ quadratically in Eq. (31). Obviously, the uncertainty of $J_{\rm sym}$ is very large and its strong dependence on the still poorly constrained $K_{\rm sym}$ partially explains why constraining $J_{\rm sym}$ is difficult. Moreover, the last term in Eq. (31), namely, $I_0L/3K_0 \approx I_0/12$, also contributes significantly to the uncertainty of $J_{\rm sym}$ because we have little knowledge on I_0.

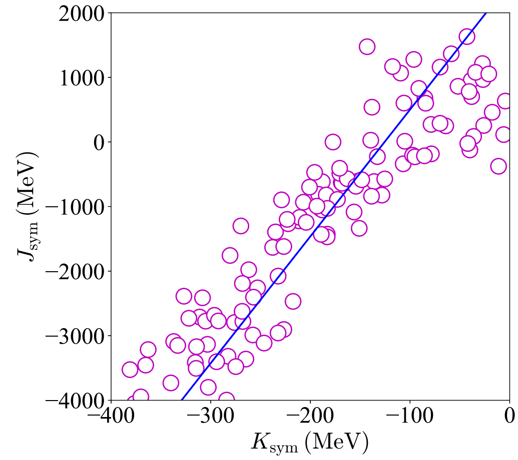

FIG. 5. Correlation between $J_{\rm sym}$ and $K_{\rm sym}$ according to the relation (31).

One can obtain the fitting parameters p and q appearing in the linear fit $J_{\rm sym} \approx pK_{\rm sym} + q$ by the same method adopted in the analysis of the correlation between $K_{\rm sym}$ and L. Taking $n = 10^4$ independent runs of the simulation with each simulation $m = 10^2$ points, we obtain $\overline{p} \approx 19.65 \pm 1.38$ and $\overline{q} \approx 2550 \pm 342$ MeV. The large slope $\overline{p}$ means that $J_{\rm sym}$ is very sensitive to the change in $K_{\rm sym}$. For example, $J_{\rm sym}$ is 979 MeV (193 MeV) if $K_{\rm sym}$ is taken as -80 MeV (-120 MeV). Thus, although the change in $K_{\rm sym}$ is only 40 MeV, the corresponding change in $J_{\rm sym}$ is about -786 MeV. This shows again that obtaining the constraint on $J_{\rm sym}$ is very difficult unless $K_{\rm sym}$ is very well constrained. It is interesting to note that the strong positive correlation between $J_{\rm sym}$ and $K_{\rm sym}$ was also reported in Ref. [25] (see Fig. 7 therein).

IV. SUMMARY

In summary, the unbound nature of PNM requires a sum rule linking intrinsically the ANM EOS parameters independent of any theory. By analyzing this sum rule at different orders of δ^2, we found several novel correlations relating the characteristics of the SNM EOS with those of nuclear symmetry energy. In particular, at the lowest-order of approximations, the bulk parts of the slope L, the curvature $K_{\rm sym}$, and the skewness $J_{\rm sym}$ of the symmetry energy are found to be $L \approx K_0/3$, $K_{\rm sym} \approx LJ_0/2K_0$, and $J_{\rm sym} \approx I_0L/3K_0$, respectively. High-order corrections to these simple relations can be written in terms of the small ratios of high-order EOS parameters. The resulting intrinsic correlations among the magnitude S, the slope L, the curvature $K_{\rm sym}$, and the skewness $J_{\rm sym}$ of the nuclear symmetry energy reproduce very nicely their empirical correlations from various microscopic nuclear many-body theories and phenomenological models in the literature.

The unbound nature of PNM is fundamental and the required intrinsic correlations among the characteristics of ANM are general. Because the EOS of PNM is the sum of two sectors, the SNM EOS and different orders of nuclear symmetry energy from expanding the ANM EOS $E(\rho, \delta)$ in even powers of δ, the vanishing pressure of PNM at zero density naturally relates the characteristics of the two sectors. While much progress has been made by the nuclear physics community in probing separately characteristics of the two parts of the ANM EOS, very little is known about the correlations between the characteristics of the SNM and those of the symmetry energy. The intrinsic correlations among the characteristics of the ANM EOS provide a novel and model-independent tool not only for consistency checks but also for investigating the poorly known high-density properties of neutron-rich matter by using those with smaller uncertainties.

ACKNOWLEDGMENTS

This work is supported in part by the U.S. Department of Energy, Office of Science, under Grant No. DE-SC0013702, and the CUSTIPEN (China-U.S. Theory Institute for Physics with Exotic Nuclei) under U.S. Department of Energy Grant No. DE-SC0009971.

[1] P. Ring and P. Schuck, *The Nuclear Many-Body Problem* (Springer, Berlin, 1980).
[2] P. Danielewicz, R. Lacey, and W. G. Lynch, Science **298**, 1592 (2002).
[3] V. Baran, M. Colonna, V. Greco, and M. Di Toro, Phys. Rep. **410**, 335 (2005).
[4] B. A. Li, L. W. Chen, and C. M. Ko, Phys. Rep. **464**, 113 (2008).
[5] B. A. Li, À. Ramos, G. Verde, and I. Vidaña, Eur. Phys. J. A **50**, 9 (2014).
[6] G. Colo, U. Garg, and H. Sagawa, Eur. Phys. J. A **50**, 26 (2014).
[7] M. Baldo and G. F. Burgio, Prog. Part. Nucl. Phys. **91**, 203 (2016).
[8] M. Oertel, M. Hempel, T. Klähn, and S. Typel, Rev. Mod. Phys. **89**, 015007 (2017).
[9] U. Garg and G. Colò, Prog. Part. Nucl. Phys. **101**, 55 (2018).
[10] K. Hebler, J. D. Holt, J. Menendez, and A. Schwenk, Annu. Rev. Nucl. Part. Sci. **65**, 457 (2015).
[11] J. Carlson, S. Gandolfi, F. Pederiva, S. C. Pieper, R. Schiavilla, K. E. Schmidt, and R. B. Wiringa, Rev. Mod. Phys. **87**, 1067 (2015).
[12] B. Friedman and V. J. Pandharipande, Nucl. Phys. A **361**, 502 (1981).
[13] W. D. Myers and W. J. Swiatecki, Acta Phys. Pol. B **26**, 111 (1995).
[14] A. Schwenk and C. J. Pethick, Phys. Rev. Lett. **95**, 160401 (2005).
[15] A. Gezerlis and J. Carlson, Phys. Rev. C **81**, 025803 (2010).
[16] S. Huth, C. Wellenhofer, and A. Schwenk, Phys. Rev. C **103**, 025803 (2021).
[17] M. J. H. Ku, A. T. Sommer, L. W. Cheuk, and M. W. Zwierlein, Science **335**, 563 (2012).
[18] I. Tews, J. M. Lattimer, A. Ohnishi, and E. E. Kolomeitsev, Astrophys. J. **848**, 105 (2017).
[19] S. Giorgini, L. P. Pitaevskii, and S. Stringari, Rev. Mod. Phys. **80**, 1215 (2008).
[20] F. J. Fattoyev, C. J. Horowitz, J. Piekarewicz, and G. Shen, Phys. Rev. C **82**, 055803 (2010).
[21] F. J. Fattoyev, W. G. Newton, J. Xu, and B.-A. Li, Phys. Rev. C **86**, 025804 (2012).
[22] B. A. Li, B. J. Cai, L. W. Chen, and J. Xu, Prog. Part. Nucl. Phys. **99**, 29 (2018).
[23] W. G. Newton, M. Gearheart, and B. A. Li, Astrophys. J. Suppl. Ser. **204**, 9 (2013).
[24] W. G. Newton and G. Crocombe, arXiv:2008.00042.
[25] J. Margueron and F. Gulminelli, Phys. Rev. C **99**, 025806 (2019).
[26] X. Roca-Maza, M. Brenna, G. Colo, M. Centelles, X. Vinas, B. K. Agrawal, N. Paar, D. Vretenar, and J. Piekarewicz, Phys. Rev. C **88**, 024316 (2013).
[27] K. Lida and K. Oyamatsu, Eur. Phys. J. A **50**, 42 (2014).
[28] C. Providência *et al.*, Eur. Phys. J. A **50**, 44 (2014).
[29] C. Mondal, B. K. Agrawal, J. N. De, S. K. Samaddar, M. Centelles, and X. Vinas, Phys. Rev. C **96**, 021302(R) (2017).
[30] J. W. Holt and Y. Lim, Phys. Lett. B **784**, 77 (2018).
[31] B. A. Li and M. Magno, Phys. Rev. C **102**, 045807 (2020).
[32] H. Gil, Y. M. Kim, P. Papakonstantinou, and C. H. Hyun, arXiv:2010.13354.
[33] B. A. Li, P. G. Krastev, D. H. Wen, and N. B. Zhang, Eur. Phys. J. A **55**, 117 (2019).
[34] B. J. Cai and L. W. Chen, Nucl. Sci. Tech. **28**, 185 (2017).
[35] L.-W. Chen, B.-J. Cai, C. M. Ko, B.-A. Li, C. Shen, and J. Xu, Phys. Rev. C **80**, 014322 (2009).
[36] B. A. Li and X. Han, Phys. Lett. B **727**, 276 (2013).
[37] C. Drischler, R. J. Furnstahl, J. A. Melendez, and D. R. Phillips, Phys. Rev. Lett. **125**, 202702 (2020).
[38] B. A. Li, C. M. Ko, and W. Bauer, Int. J. Mod. Phys. E **7**, 147 (1998).
[39] B. J. Cai and L. W. Chen, Phys. Rev. C **85**, 024302 (2012).
[40] C. Gonzalez-Boquera, M. Centelles, X. Vinas, and A. Rios, Phys. Rev. C **96**, 065806 (2017).
[41] J. Pu, Z. Zhang, and L. W. Chen, Phys. Rev. C **96**, 054311 (2017).
[42] C. H. Lee, T. T. S. Kuo, G. Q. Li, and G. E. Brown, Phys. Rev. C **57**, 3488 (1998).
[43] P. Russotto *et al.*, Phys. Rev. C **94**, 034608 (2016).
[44] D. H. Youngblood, H. L. Clark, and Y.-W. Lui, Phys. Rev. Lett. **82**, 691 (1999).
[45] S. Shlomo, V. M. Kolomietz, and G. Colo, Eur. Phys. J. A **30**, 23 (2006).
[46] L. W. Chen and J. Z. Gu, J. Phys. G: Nucl. Part. Phys. **39**, 035104 (2012).
[47] W. J. Xie and B. A. Li, J. Phys. G: Nucl. Part. Phys. **48**, 025110 (2021).
[48] W. J. Xie and B. A. Li, Astrophys. J. **899**, 4 (2020).
[49] W. J. Xie and B. A. Li, Astrophys. J. **883**, 174 (2019).
[50] A. Blum, J. Hopcroft, and R. Kannan, *Foundations of Data Science* (Cambridge University Press, Cambridge, England, 2020), Chap. 1.
[51] T. Malik, B. K. Agrawal, C. Providencia, and J. N. De, Phys. Rev. C **102**, 052801(R) (2020).
[52] T. Malik, N. Alam, M. Fortin, C. Providencia, B. K. Agrawal, T. K. Jha, B. Kumar, and S. K. Patra, Phys. Rev. C **98**, 035804 (2018).
[53] R. Somasundaram, C. Drischler, I. Tews, and J. Margueron, arXiv:2009.04737.